Chemical Engineering Journal 152 (2009) 440–448

Contents lists available at ScienceDirect

Chemical Engineering Journal

journal homepage: www.elsevier.com/locate/cej

Copper and chromium(VI) removal by chitosan derivatives—Equilibrium and kinetic studies

George Z. Kyzas, Margaritis Kostoglou, Nikolaos K. Lazaridis*

Division of Chemical Technology, School of Chemistry Aristotle University, GR-541 24, Thessaloniki, Greece

ARTICLE INFO

Article history:
Received 5 December 2008
Received in revised form 24 April 2009
Accepted 1 May 2009

Keywords:
Copper
Hexavalent chromium
Chitosan
Sorption
Isotherms
Cross-linking
Kinetic model
Diffusion-reaction model (DIFRE)

ABSTRACT

Chitosan sorbents, cross-linked and grafted with amido or carboxyl groups, were prepared and their sorption properties for Cu(II) and Cr(VI) uptake were studied. Equilibrium sorption experiments were carried out at different pH values and initial ion concentrations. The equilibrium data were successfully fitted to the Langmuir–Freundlich (L–F) isotherm. The calculated maximum sorption capacity of the carboxyl-grafted sorbent for Cu(II) was found to be 318 mg/g at pH 6, while the respective capacity for Cr(VI) uptake onto the amido-grafted sorbent was found to be 935 mg/g at pH 4. Thermodynamic parameters of the sorption process such as ΔG^0, ΔH^0, and ΔS^0 were also calculated. The experimental kinetic data were successfully fitted to a novel phenomenological diffusion-reaction model (DIFRE), which combines: (i) mass transfer of the metal ions from the bulk solution on the sorbent surface; (ii) diffusion of the ions through the swollen polymer particle; and (iii) instantaneous local chelation (for cations) or electrostatic attraction (for anions) on the amino groups of the polymer. The regeneration of sorbents was affirmed in four sequential cycles of sorption–desorption experiments, without significant loss in sorption capacity.

1. Introduction

One of the most naturally abundant and cheap biopolymers is chitosan, which has been studied for its metal-chelating properties for the removal of various metal ions from wastewaters [1–3]. It is a hydrophilic, nontoxic, biodegradable, and biocompatible material with ability to form complexes with metals [4]. This could be easily explained by the presence of amino groups in the polymer matrix, which can interact with metal ions in the solution by ion exchange and complexation reactions [5]. The high content of amino groups also makes possible many chemical modifications in the polymer with the purpose of improving its sorptive features, such as selectivity and adsorption capacity [6]. Grafted functional groups such as carboxyl, hydroxyl, sulfate, phosphate, and amino groups on the biosorbents have been reported to be responsible for metal binding [7].

Although the interaction of metal ions with chitosan based sorbents has been studied extensively and there are several semi-phenomenological modeling approaches, there is still a lack of a unified mechanistic modeling approach to the subject [2]. The development of such a model requires extended experimental results on the interaction between swelling and adsorption kinetics. Given the lack of such data, only some aspects of the sorption process will be studied here. A first observation is that the chitosan derivatives of the present study have a very low surface area (0.1–1 m^2/g) [8]. So, it is not clear how it is distributed on the particle volume (surface roughness or uniform porosity). It does not really matter, because it is believed that after the first stages of swelling, the porous structure disappears and the swollen particle takes the form of a homogeneous gel material, in which the water has to diffuse to achieve further swelling until equilibrium is established. Then, the metal ions are diffused into the swollen polymer phase and are incorporated (adsorbed) on the polymer by (i) chelation on the amine groups in the case of cations [2], and (ii) by electrostatic attraction in the case of anions [2]. The kinetics of the whole process has been modeled in two distinct ways: (i) based on diffusion [9], and (ii) based on the global chelation reaction [10]. The reaction typically is assumed to be reversible or second-order irreversible. It is noted that in studies in which the second-order kinetics is used [11], it is not clear whether the sorption occurs on the whole particle volume or only on some depth under the particle surface.

In this study, raw chitosan has been suitably modified by cross-linking with glutaraldehyde to increase the resistance to chemical and biological degradation, followed by grafting reactions introducing either carboxyl or amido groups to increase its sorption capacity. A previously published work affirmed the use of the prepared materials as biosorbents for basic dyes, presenting high sorption capacities equal to 455 mg/g (≈1.068 mmol/g) [8].

However, there is no study regarding the sorption of Cu(II) and Cr(VI) onto carboxyl- or amido-grafted chitosan sorbents. In gen-

---

* Corresponding author. Tel.: +30 32310 997807; fax: +30 32310 997759.
E-mail address: nlazarid@chem.auth.gr (N.K. Lazaridis).

1385-8947/$ – see front matter © 2009 Elsevier B.V. All rights reserved.
doi:10.1016/j.cej.2009.05.005

Table 1
Comparative table for the sorption capacities of cross-linked chitosan derivatives.

Metal	Sorbent	pH	Isotherm model	Q_{max} (mg/g)	Reference
Cu(II)	Chitosan	6	L	60	[13]
	Chitosan	5	L	200	[14]
	Chitosan	4.5	L, F	125	[15]
	Chitosan-g-PEI	4.5	L, F	84	[15]
	Chitosan-g-BPMAMF	6	L, F	109	[16]
	Chitosan	6	L	80	[17]
	Chitosan	6	L–F	67	[10]
	Ch	6	L–F	208	This study
	Ch-g-Aa	6	L–F	318	This study
	Ch-g-Aam	6	L–F	166	This study
Cr(VI)	Chitosan	4	L	78	[17]
	Chitosan	4	L	40	[18]
	Chitosan xanthated	3	L	256	[19]
	Chitosan	4	L, F	215	[20]
	Chitosan	4	L	154	[21]
	Ch	4	L–F	655	This study
	Ch-g-Aa	4	L–F	518	This study
	Ch-g-Aam	4	L–F	935	This study

Abbreviations: Chitosan-g-PEI, chitosan grafted with polyethyleneinime; Chitosan-g-BPMAMF, chitosan grafted with 2[-bis-(pyridylmethyl)aminomethyl]-4-methyl-6-formylphenol; L, Langmuir; F, Freundlich; L–F, Langmuir–Freundlich.

eral, the sorption capacities of cross-linked chitosan, as reported in literature, ranged from 60 to 200 mg/g for Cu(II) and 40–250 mg/g for Cr(VI) [2,12]. Table 1 briefly reports the maximum sorption capacities presented by cross-linked chitosan sorbents that were cited for uptake of Cu(II) and Cr(VI) ions, with the corresponding references. A direct comparison of experimental data is not possible since experimental conditions (pH, sorbent's particle size, conditioning, and composition of the solution) are not systematically the same. In our study, we achieved an improvement of the sorption capacities of the prepared sorbents reaching 318 mg/g in the case of Cu(II) uptake by carboxyl-grafted chitosan derivative and 935 mg/g in the case of Cr(VI) uptake by amido-grafted chitosan derivative.

Sorption experiments for the removal of either Cu(II) or Cr(VI) were conducted to evaluate the effectiveness of the prepared materials, while Fourier Transform Infrared spectroscopy (FTIR) was used to verify the interaction between metals and chitosan. Furthermore, a novel kinetic model was also proposed to fit the experimental data. The effect of pH on desorption of ions by loaded chitosan sorbents and the regeneration of these sorbents carrying out sequential cycles of sorption–desorption experiments were also studied.

2. Materials and methods

2.1. Materials

High molecular weight chitosan was obtained from Sigma–Aldrich and purified by extraction with acetone in a Soxhlet apparatus for 24 h, followed by drying under vacuum at 25 °C. The average molecular weight was estimated at 3.55×10^5 and the degree of deacetylation was 82 wt% [22]. Acrylamide 97% p.a. was purchased from Sigma–Aldrich and used without further purification. Acrylic acid received from Merck was purified by distillation under vacuum. Potassium persulfate obtained from Merck was used as received. Glutaraldehyde, 50 wt% in water, was used as reagent grade from Sigma–Aldrich, while all the solvents were of analytical grade. $CuSO_4 \cdot 5H_2O$ (Fluka, 98% purity) and $K_2Cr_2O_7$ (Fluka, puriss. p.a. $\geq$ 99.0%) were used for the preparation of Cu(II) and Cr(VI) stock solutions, respectively.

2.2. Preparation of biosorbents

The preparation of the cross-linked and grafted chitosan derivative with poly(acrylamide) (noted as *Ch-g-Aam*) and poly(acrylic acid) (noted as *Ch-g-Aa*) has been published in our previous study [8]. Briefly, raw powder of chitosan was initially dissolved in aqueous solution of acetic acid followed by monomer grafting (poly(acrylamide) or poly(acrylic acid)) and then by heterogeneously chemical cross-linking with glutaraldehyde, rendering the substances insoluble in acidic media. Given that chitosan is very stable in alkaline and neutral solutions, but soluble in acidic pHs [22,23], we have cross-linked the chitosan sorbents to make them resistant and insoluble in all pH conditions. Non-grafted cross-linked chitosan (*Ch*) was used as reference in all experiments.

The final grafting percentages, determined on the basis of the percentage weight increase of the final product relative to the initial weight of the chitosan ($\%G = 100 \times (W_2 - W_1)/W_1$, where W_1 and W_2 denote the weight of the initial dry chitosan, grafted chitosan after extraction and drying, respectively), were estimated at approximately 230% poly(acrylamide) for *Ch-g-Aam* and 300% poly(acrylic acid) for *Ch-g-Aa*. All the prepared products were ground to fine powders (100 ± 15 μm).

2.3. FTIR spectroscopy

Loaded with metal ions and non-loaded sorbents were analyzed with a PerkinElmer FTIR spectrometer, model Spectrum 1000, using KBr pellets. The resolution for each spectrum was 2 cm^{-1} and the number of co-added scans was 64. The spectra presented are baseline corrected and converted to the absorbance mode.

2.4. Sorption–desorption experiments

Experiments for the effect of pH on Cu(II) and Cr(VI) sorption were performed by mixing 0.05 g of sorbent with 50 mL of an aqueous metal ion solution of 100 mg/L. The pH was continuously monitored and adjusted by micro-additions of 0.1 M NaOH or 0.1 M HCl to keep it constant to the various predetermined values, during the sorption time. The solutions were agitated at 160 rpm in a temperature controlled shaker at 25 °C (Julabo SW-21C) for 24 h (contact time).

Equilibrium studies were also carried out by mixing 0.05 g of sorbent with fixed volumes of solutions (50 mL) containing different initial concentrations of Cu(II) or Cr(VI) (20–500 mg/L) at different constant temperatures (25, 45, 65 °C). The suspensions were shaken for 24 h at 160 rpm, under optimum pH conditions.

Kinetic experiments were performed by mixing 0.05 g of sorbent with 50 mL of an aqueous solution of Cu(II) (pH 6) or Cr(VI) (pH 4) of 100 mg/L. The mixture was shaken at 160 rpm for 24 h at 25 °C. Samples were collected at fixed intervals (5, 10, 20, 30 min, 1, 2, 3, 4, 5, 6, 12, 24 h) and then were analyzed spectrophotometrically.

After sorption experiments (initial concentration of ions = 100 mg/L, 25 °C, 24 h, pH 6 for Cu and pH 4 for Cr(VI), 160 rpm), the ion-loaded sorbents were collected and filtered by 0.45 μm pore-size membranes. The desorption experiments were realized by mixing the collected amount of loaded chitosan with aqueous solutions of 50 mL at pH range 2–12 (25 °C, 24 h, 160 rpm). As it was described in the sorption experiments, after 24 h of shaking at the aforementioned conditions, the samples were collected and spectrophotometric analysis revealed the optimum desorption pH value. In order to determine the reusability of the prepared sorbents, consecutive sorption–desorption cycles were realized following the experimental procedures described above.

2.5. Analysis

Samples of the Cr(VI) solution were collected at pre-determined time intervals, filtered and analyzed using a UV–Vis Spectrophotometer (model U-2000, Hitachi), at $\lambda_{\max} = 540$ nm, according to the 1,5-diphenyl-carbazide method [24]. The respective samples of the solution of Cu(II) were analyzed by atomic absorption spectroscopy, using an Atomic Absorption Spectrophotometer (PerkinElmer AAnalyst 400) composed of FIAS 100 Flow Injection System. Due to the sensitivity of the instrument, the samples with high residual ion concentrations were diluted before the measurement. The aforementioned dilution was taken into account for all the calculations.

2.6. Equilibrium model

The experimental equilibrium data were fitted to the Langmuir–Freundlich isotherm (L–F, Eq. (1)), which is essentially a Freundlich isotherm and approaches a maximum at high concentrations [25]:

$$Q_e = \frac{Q_{\max}(K_{LF}C_e)^b}{1+(K_{LF}C_e)^b} \tag{1}$$

where Q_e (mg/g) is the equilibrium metal ion concentration in the solid phase; $Q_{\max}$ (mg/g) is the maximum amount of sorption; K_{LF} $(\text{mL/mg})^{1/b}$ is the Langmuir–Freundlich constant; b is the Langmuir–Freundlich heterogeneity constant. This isotherm corresponds to a generalized equilibrium condition for the chelation reaction or for the electrostatic attraction dominated adsorption.

The equilibrium metal ion concentration in the solid phase Q_e, was calculated using the mass balance equation:

$$Q_e = \frac{(C_{bo} - C_e)\cdot V}{m} \tag{2}$$

where m (g) is the mass of sorbent; V (L) the volume of sorbate; C_{bo} and C_e (mg/L) the initial and equilibrium ion concentrations, respectively.

The fact that almost all the migrating metal ions are in the adsorbed state can be confirmed by a simple computation. The mass of metal which is depleted from the solution at equilibrium is mQ_e. In the present study, it is assumed that all this mass is in the adsorbed state. The mass which is entrapped in the sorbent matrix (but not adsorbed) is $(m/\rho)\varphi C_e$, where $\varphi < 1$ is the liquid volume fraction of the particle and ρ is the density of sorbent. The ratio of the entrapped to the depleted metal mass is given as $\varphi C_e/(\rho Q_e)$. This quantity is smaller than 0.001 in all of our experiments confirming that the depleted metal is in the adsorbed state.

2.7. Kinetic model

Many papers have been published regarding the kinetic analysis of metal ion sorption and especially of Cu(II) and Cr(VI) onto chitosan [13,18,26–29]. In literature, standard kinetic equations such as pseudo first-, second-order, and Elovich equation were used to fit the experimental kinetic data [30–34].

In the present study, the diffusion-based and the reaction-based models are combined by assuming a very fast local chelation (immobilization) process with respect to the diffusion process. This means that there is always equilibrium between the free and the bound metal ions on amines metal ions. Of course, there will be some interference between the swelling and the sorption processes, because the diffusion kinetics depend on the local water content [35]. The pure sorption model would be valid only for sorbent particles left in pure water with enough time to achieve the maximum degree of swelling (or alternatively a swelling process much faster than the sorption process). In the present experiments, the sorbent particles have not been previously exposed to water, so an interference of the swelling and sorption processes is possible. At this point it will be ignored due to the absence of data, so the water content and the diffusivity will be assumed uniform throughout the particle.

The proposed model contains mass transfer of the metal ions from the bulk solution onto the surface of the sorbent particles, diffusion of the ions through the swollen polymer particle and instantaneous (equilibrium) local chelation or electrostatic immobilization on the amino groups of the polymer. Although the process is conceptually different from the sorption in porous sorbents [36], from the mathematical point of view the model of the above process is similar to the model of pore-diffusion dominated sorption on porous sorbents, with the chelation or electrostatic attraction equilibrium playing the role of the usual sorption–desorption equilibrium. More specifically, by assuming that the concentration of the free ions is much lower than that of bounded ions the mathematical model takes the form:

$$\frac{\partial q}{\partial t} = \frac{1}{r^2}\frac{\partial}{\partial r}r^2 D(C)\frac{\partial q}{\partial r} \tag{3}$$

with the following boundary conditions:

Spherical symmetry

$$\left(\frac{\partial q}{\partial r}\right)_{r=0} = 0 \tag{4}$$

Bulk to particle mass transfer

$$K_m(C_b - C) = \rho_\rho D\left(\frac{\partial q}{\partial r}\right)_{r=R} \tag{5}$$

where t is the time; r is the radial coordinate in the spherical particle; q is the local adsorbed ion concentration (mass of ions per mass of sorbent); C_b is the mass concentration of the metal ions in the solution; K_m is the mass transfer coefficient from the bulk solution to the particle; R is the particle radius of the sorbent; ρ_ρ is its density.

The equilibrium relation between free and adsorbed ions is $q = f(C)$ where C is the concentration of free ions in the liquid phase of the particle. The concentration C in Eqs. (3) and (5) can be found by inverting the relation $q = f(C)$. The diffusivity D is an effective diffusivity which combines the diffusion and adsorption (chelation or electrostatic) phenomena and is given through the relation:

$$D = \frac{D_\rho}{\rho_p f'(C)} \tag{6}$$

The prime in the above equation denotes the differentiation of a function with respect to its argument. The diffusivity D_ρ depends in principle on the structure of the swelled particle so it can be considered as a constant since a uniform water distribution in the particle has been already assumed. The average concentration of the adsorbed species can be computed by the relation:

$$q_{ave} = \frac{3}{R^3}\int_0^R qr^2 dr \tag{7}$$

In the case of batch experiments the concentration of the solute in bulk liquid C_b decreases due to its sorption by the sorbent. Therefore, the evolution of the C_b must be taken into account by the model. The easier way to do this is to consider a global mass balance of the sorbate:

$$C_b = C_{b_0} - \frac{m}{V} q_{ave} \tag{8}$$

The Langmuir–Freundlich expression in Eq. (1) found from equilibrium experiments must be used for the function f(C) (using C in place of C_e and q in place of Q_e) in order to describe appropriately the experimental data. This non-linear equilibrium relation makes the whole problem non-linear precluding the use of any analytical solution technique or semi-analytical dimensionality reduction techniques [37,38]. Thus, the system of Eqs. (3)–(8) is solved numerically employing a second-order finite difference discretization in the radial direction and an explicit Ordinary Differential Equations (ODEs) integrator with self-adjusting step for the solution of the system of resulting ODEs (method of lines) [39]. The non-linearity in boundary condition (Eq. (5)) is treated by solving the corresponding algebraic equation by the Newton–Raphson technique at each time step.

3. Results and discussion

3.1. Effect of pH on sorption

The effect of pH on the sorption of copper ions onto the prepared chitosan sorbents is depicted in Fig. 1a. At pH 2 the copper uptake was low, while a slight increase was observed in the range of 2–4, followed by a sharp increase at higher pHs. In alkaline conditions, complete sorption was observed, but in this pH region the copper removal originates form precipitation ($Cu(OH)_2$) rather than from sorption [1]. In general, for the whole pH range the sorptive behavior of the prepared materials followed the order: *Ch-g-Aa* > *Ch* > *Ch-g-Aam*. Therefore, in order to guarantee the sorption mechanism and presence of copper ions in the suspension avoiding precipitation, pH 6 was selected for the further experimental procedures (kinetics and thermodynamic analysis).

The effect of pH on the sorption of chromium ions onto the prepared chitosan sorbents is depicted in Fig. 1b. Contrary to copper ions, high sorption percentages were observed in the acidic pH region. At pH 4 there was a sharp increase. In the case of chromium ions, at low pH (2) the uptake ranges in high levels (~70%). While increasing the pH, a maximum removal of chromium ions is observed at pH 4 (77%, *Ch*; 90%, *Ch-g-Aam*; 67%, *Ch-g-Aa*). Then, for higher pH values (pH >6), a decrease in sorption is presented. The order of chromium ions uptakes was the same for all the pH values: *Ch-g-Aam* > *Ch* > *Ch-g-Aa*. Similar pH behavior (higher sorption at low pH and lower uptakes with the increase of pH) was observed by other researchers [13,17,18,28,29].

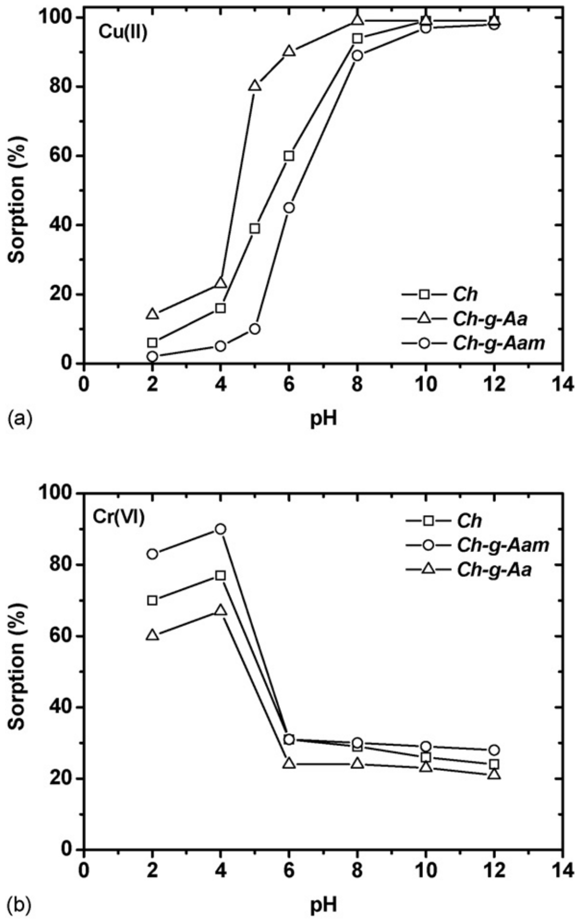

Fig. 1. Effect of pH on the sorption of: (a) Cu(II); (b) Cr(VI).

3.2. Equilibrium—thermodynamic studies

Fig. 2a and b presents the sorption capacities versus equilibrium concentrations in the liquid phase for Cu(II) and Cr(VI) removal, respectively. The data were successfully fitted to the L–F model (R^2 = 0.996–0.999) and the resulted parameters are given in Table 2. The data showed an increase in the amount of ion sorbed, when the initial ion concentration increases. The sorption capacities for Cu(II) followed the order *Ch-g-Aa* > *Ch* > *Ch-g-Aam* (318, 208, 166 mg/g at 25 °C, respectively), while the respective order for Cr(VI) was: *Ch-g-Aam* > *Ch* > *Ch-g-Aa* (935, 655, 518 mg/g at 25 °C, respectively). An increase in sorption capacity was presented with the increase of temperature from 25 to 65 °C, indicating the endothermic nature of the process. In the case of Cu(II), the maximum sorption capacity was calculated for *Ch-g-Aa* (397 mg/g, 65 °C), while for Cr(VI), the sorption capacity of *Ch-g-Aam* was 1254 mg/g at 65 °C.

The thermodynamic equilibrium constant K_c for the sorption process was determined by plotting ln(Q_e/C_e) versus Q_e and extrapolating to zero Q_e [40–42]. Regression straight lines are fitted through the data points by the least squares method, and their intersections with the vertical axis give the value of K_c. The increasing sorption with increasing temperature can be explained on the basis of thermodynamic parameters such as changes in free energy (ΔG^0), enthalpy (ΔH^0), and entropy (ΔS^0), which are estimated from the following relationships:

$$\Delta G^0 = -RT \cdot \ln(K_c) \tag{9}$$

$$\ln(K_c) = -\frac{\Delta H^0}{R} \cdot \frac{1}{T} + \frac{\Delta S^0}{R} \tag{10}$$

where T (K) is the temperature; R (=8.314 × 10^{-3} kJ/mol K) is the universal gas constant. ΔH^0 and ΔS^0 were obtained from the slope and intercept of Van't Hoff plots of ln(K_c) versus 1/T (R^2 > 0.95).

Table 2
Equilibrium and thermodynamic parameters for the sorption of Cu(II) and Cr(VI) onto chitosan derivatives.

Sorbent	Sorbate	L–F isotherm model					Thermodynamics				
		T (°C)	Q_{max} (mg/g)	K_{LF} ((mL/mg)$^{1/b}$)	b	R^2	ΔG^0 (kJ/mol)	ΔH^0	ΔS^0 (kJ/mol K)	$\Delta H^0{}_{net}$ (kJ/mol)	$T\Delta S^0$
Ch	Cu(II)	25	208	2.33	0.808	0.999	−3.34	15.18	0.062	79.58	19.72
		45	222	3.79	0.844	1.000	−4.01				
		65	233	3.64	0.794	1.000	−5.15				
Ch-g-Aam	Cu(II)	25	166	1.49	0.822	1.000	−1.14	15.73	0.057	80.13	18.13
		45	176	1.46	0.780	1.000	−2.41				
		65	184	1.91	0.790	1.000	−2.99				
Ch-g-Aa	Cu(II)	25	318	0.69	0.492	0.991	−11.13	32.89	0.149	97.29	47.38
		45	381	0.40	0.448	0.993	−13.17				
		65	397	0.39	0.424	0.994	−15.01				
Ch	Cr(VI)	25	655	20.53	1.133	0.998	−4.31	11.41	0.053	−851.8	16.85
		45	719	9.99	1.030	0.998	−4.92				
		65	804	3.57	0.900	0.999	−5.67				
Ch-g-Aam	Cr(VI)	25	935	1.25	0.783	1.000	−6.65	19.14	0.086	−844.1	27.35
		45	982	1.14	0.749	1.000	−7.68				
		65	1254	0.27	0.615	1.000	−8.92				
Ch-g-Aa	Cr(VI)	25	518	68.00	1.318	0.999	−2.31	14.02	0.055	−849.2	17.49
		45	558	44.51	1.254	0.998	−3.11				
		65	613	31.11	1.205	0.997	−3.98				

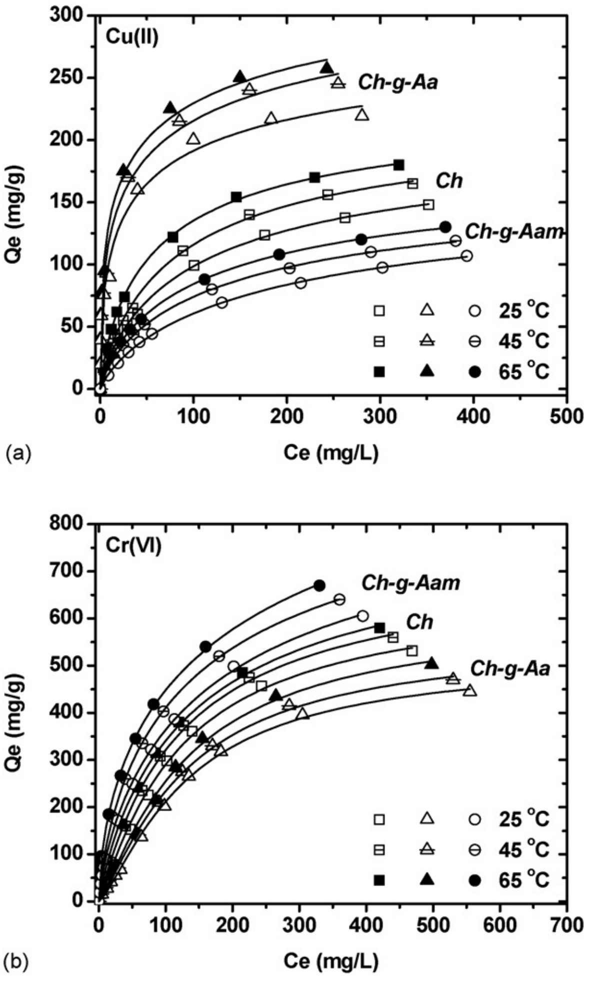

Fig. 2. Sorption isotherms fitted to the L–F model at different temperatures for: (a) Cu(II) removal; (b) Cr(VI) removal.

The apparent heat of adsorption in aqueous solutions ΔH^0 is the resultant of the net heat of adsorption $\Delta H^0{}_{net}$, heat of solution of adsorbate ΔH^{sol} and the heat of sorption of water, ΔH^w, i.e.:

$$\Delta H^0 = \Delta H^0_{net} - \Delta H^{sol} - f\Delta H^w \tag{11}$$

where f is the exchange of number of moles of water per mole of adsorbate. ΔH^w is normally assumed to be zero and ΔH^{sol} of the adsorbate in the solvent may be calculated from the heats of formation of anions and cations in aqueous solution, i.e. +64.4 kJ/mol for $Cu^{2+}(aq)$ and −863.2 kJ/mol for $CrO_4{}^{2-}(aq)$ [43]. The resulting thermodynamic parameters are given in Table 2. Both Cu(II) and Cr(VI) removals were characterized as endothermic processes due to their positive values of ΔH^0. Furthermore, an increased trend in the negative values of ΔG^0 values revealed an increased trend in the degree of spontaneity and feasibility of metal sorption. The positive values of ΔS^0 show the increased randomness at the solid/solution interface during the sorption of metal ions (either Cu(II) or Cr(VI)) on chitosan and also reflect the affinity of the sorbent for the metal ions under consideration [44]. During the sorption process, the coordinated water molecules, that are displaced by either Cu(II) or Cr(VI) species, gain more translational entropy than is lost by the Cu(II) or Cr(VI) species, respectively, resulting in increased randomness in the ion–chitosan interaction [40]. The adsorption process is dominated by enthalpic rather than entropic effects if $|\Delta H^0{}_{net}| > |T\cdot\Delta S^0|$. Given that for all cases the previous inequality is valid it means that the sorption procedure is enthalpic driven.

3.3. *Kinetic model*

In contrast to many studies on the quantative uptake of metal ions by chitosan, there have been infrequent reports in the literature on diffusion of metal ions through chitosan [3,45]. Fig. 3a and b depicts the kinetic behavior of the prepared materials during the sorption process of Cu(II) and Cr(VI) ions. The kinetic experimental curves have a continuous decreasing trend. At the beginning of the process (0–60 min), the removal of metal ion was realized rapidly (intense descent), followed by a milder fall reaching equilibrium at 120 min. In addition, according to these figures, the sorption of Cu(II) onto *Ch-g-Aa* was realized at a higher rate, than that of *Ch-g-Aam* and *Ch* (Fig. 3a). In contrast, *Ch-g-Aam* presents a higher kinetic rate in Cr(VI) sorption (Fig. 3b), followed by *Ch*

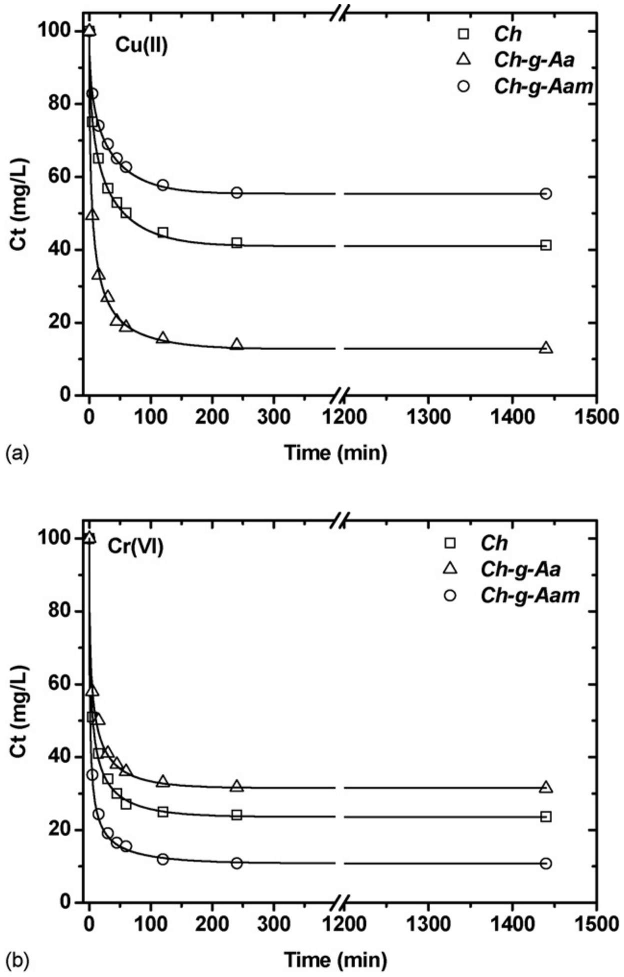

Fig. 3. Sorption kinetic data for chitosan derivatives, fitted to the proposed kinetic model: (a) Cu(II); (b)Cr(VI).

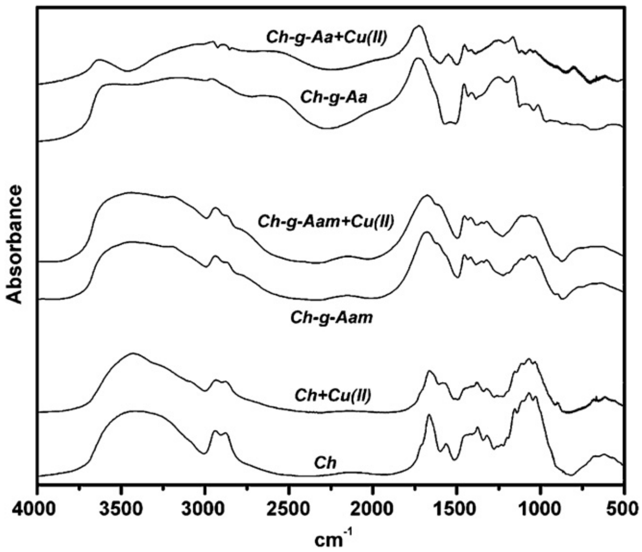

Fig. 4. FTIR spectra of chitosan derivatives for Cu(II) removal.

and *Ch-g-Aa*, respectively. Thus, the modifications of chitosan not only influence its sorption capacity, but also the kinetic rate of the process.

The resulted diffusion coefficients for Cu(II) sorption onto *Ch*, *Ch-g-Aam* and *Ch-g-Aa* were calculated by the proposed kinetic model and were equal to 3.64×10^{-10}, 2.52×10^{-10} and 9.88×10^{-10} m^2/s, respectively ($R^2 \sim 0.999$). Cr(VI) diffusion coefficients were 9.57×10^{-10}, 10.53×10^{-10} and 8.62×10^{-10} m^2/s, respectively ($R^2 \sim 0.998$). At this point, it is stressed that our proposed model is phenomenological, in contrast with the empirical models used in literature [11]. The diffusion coefficient values given in literature [17,46,47] referred to a virtual diffusion process and they have no direct relation to the actual process. Contrarily, the diffusion coefficient used by our model is the real diffusion coefficient of the ions in the swollen particle and is expected to be somewhat smaller than the diffusion coefficients of the corresponding ions in the water (due to the diffusion inhibition induced by the solid matrix of the chitosan). To confirm the above arguments, it is referenced that for Cu(II) removal the exported/calculated empirical diffusion coefficients were approximately 10^{-13} m^2/s [15–17], whereas for Cr(VI) they were about 10^{-12} m^2/s [17,46]. These coefficients are orders of magnitude smaller than the diffusion coefficients in water (7.1×10^{-10} m^2/s for Cu(II) and 1.13×10^{-9} m^2/s for Cr(VI) [48]). The diffusion coefficient from our model is between 40% and 60% of the free water diffusion coefficient as it is expected, confirming the validity of our approach. The only discrepancy is for the case of Cu(II) in *Ch-g-Aa*, where the diffusion coefficient in the particle appears to be larger than the free water diffusion coefficient. A possible explanation is the facilitation of diffusional transport due to the existence of carboxyl groups induced by the grafting of the carboxyl groups in the particular material [2].

3.4. Potential mechanism – FTIR – desorption

3.4.1. Cu(II)

The interaction between Cu(II) and the prepared sorbents has been confirmed by FTIR spectroscopy (Fig. 4). The peaks of amino groups of Cu(II)-loaded chitosan sorbents presented shifts with respect to non-loaded ones (*Ch*, 1665–1660 cm^{-1}; *Ch-g-Aam*, 1672–1674 cm^{-1}; *Ch-g-Aa*, 1674–1670 cm^{-1}), suggesting a chelated complex. All the other peaks, which are not referenced in this study, are characteristic of chitosan-based sorbents.

Furthermore, in acidic conditions all chitosan sorbents are charged positively due to the protonation of their amino groups, which induce an electrostastic repulsion to Cu(II) ions (competition existed between H$^+$ and Cu^{2+} for sorption sites onto chitosan) [1]. Therefore, the Cu(II) uptake was of low percentage. The protonation of amino groups decreases as pH increases, causing the diminishment of the above competition. Thus, uptake of Cu(II) was increased at higher pHs. The grafted amido groups derivative (*Ch-g-Aam*) presented similar sorptive behavior with *Ch*, but with lower sorption percentages for all the pH range. Due to the grafting of amido groups, a larger number of protonated amino groups exist in the chitosan matrix, causing stronger protonation (lower sorption). The grafting of carboxyl groups resulted in the induction of more negative charge (reduction of amino protonation) of the chitosan backbone, causing a stronger interaction between Cu(II) and carboxyl groups of *Ch-g-Aa* (higher sorption). The elemental analysis of *Ch-g-Aa* showed an increase in oxygen content 7.4% (w/w), with respect to ungrafted material (*Ch*), which was succeeded after 300% grafting with acrylic acid.

Desorption experiments were realized over the whole pH range. The maximum desorption of Cu(II) by the loaded chitosan sorbents were observed at pH 2 (Fig. 5). The bonds between chitosan matrix and cations of copper are weakened drastically in acidic media; the competition between H$^+$ and Cu(II) increases, resulting in the weakening of the bonds between chitosan sorptive sites and copper ions [2].

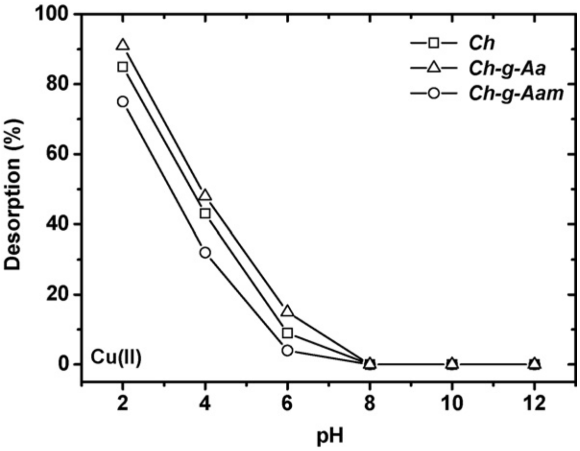

Fig. 5. Effect of pH on the desorption of Cu(II)-loaded chitosan derivatives.

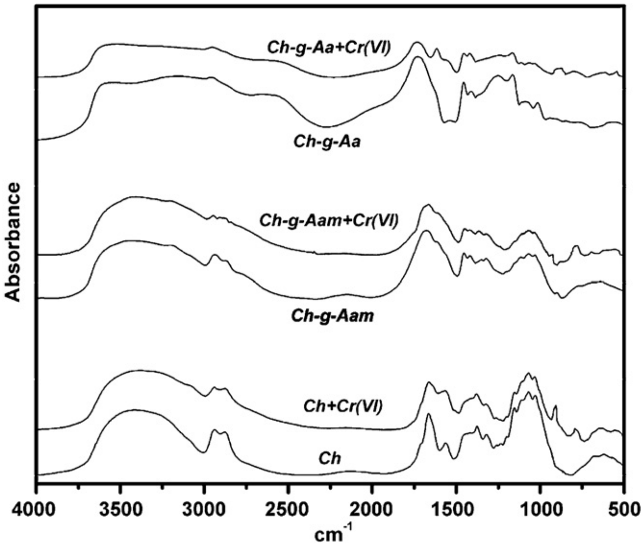

Fig. 6. FTIR spectra of chitosan derivatives for Cr(VI) removal.

3.4.2. Cr(VI)

To elucidate the mechanism of Cr(VI) sorption onto the prepared chitosan sorbents, the FTIR spectra of Cr(VI)-loaded and non-loaded materials were obtained (Fig. 6). The peaks of amino groups of Cr(VI)-loaded chitosan sorbents presented shifts with respect to non-loaded ones (*Ch*, 1665–1669 cm^{-1}; *Ch-g-Aam*, 1672–1679 cm^{-1}; *Ch-g-Aa*, 1726–1731 cm^{-1}), suggesting the electroastic interaction between $HCrO_4^-$ and amino groups of chitosan. Furthermore, two new peaks were observed in FTIR spectra of Cr(VI)-loaded sorbents attributed to Cr—O and Cr=O bonds of chromate anions confirming the sorption of Cr(VI) onto the chitosan derivatives [19]: at 789 and 910 cm^{-1}, 781 and 924 cm^{-1},779 and 907 cm^{-1} for ν_{Cr-O} and $\nu_{Cr=O}$, respectively, in the case of *Ch*, *Ch-g-Aam* and *Ch-g-Aa*.

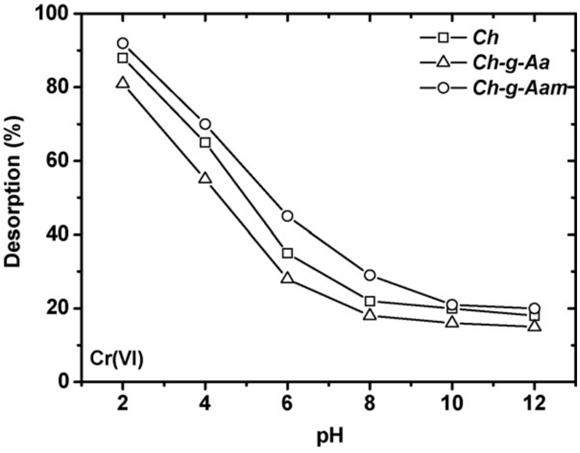

Fig. 7. Effect of pH on the desorption of Cr(VI)-loaded chitosan derivatives.

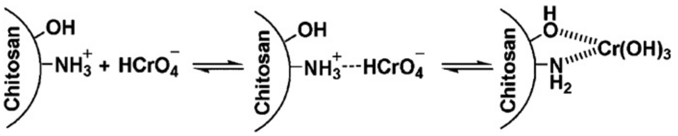

Fig. 8. Potential sorption mechanism of Cr(VI) onto chitosan derivatives.

At low pHs the sorbate is negatively charged (Cr(VI) which exists mostly as an anion ($HCrO_4^-$)) leading to the strongest electrostatic attraction between sorbent and sorbate [18,21]. The lower removal efficiency at pH 2 (with respect to pH 4) (Fig. 1b) is presumably attributed to the general instability of chitosan at such low pH values [17]. As the pH increases, a decrease in sorp-

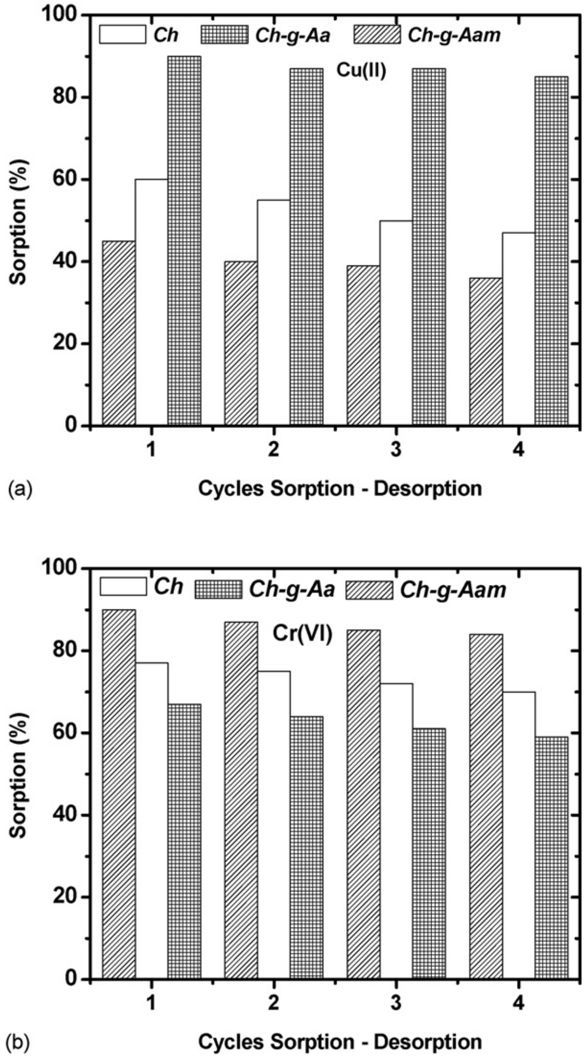

Fig. 9. Sorption–desorption cycles for chitosan sorbents: (a) Cu(II); (b) Cr(VI).

tion for all the sorbents is presented and this could be explained by the rapid changes in the protonated and deprotonated forms of the amino groups of chitosan [18]. Thus, chitosan undergoes deprotonation and the metal sorption becomes lower. The grafting of amido groups causes the increase of the protonated amino groups resulting in stronger electrostatic interactions between Cr(VI) anions and chitosan. Contrarily, the grafting of carboxyl groups onto chitosan backbone (*Ch-g-Aa*) did not improve the sorption capacity for Cr(VI) removal; the carboxyl groups reduced the positive charge of the sorbent (still positively charged), weakening the electrostatic interaction of the system sorbate-sorbent. The elemental analysis of *Ch-g-Aam* showed an increase in nitrogen content 7.1% (w/w), with respect to ungrafted material (*Ch*), which was succeeded after 230% grafting with acrylamide. However, this increase in binding sites is not fully active since the materials were cross-linked. More details about the functional groups could be given after appropriate acid-base titration studies.

The maximum desorption of Cr(VI) by the loaded sorbents was observed in acidic conditions (pH 2) (Fig. 7). A potential explanation is that initially Cr(VI) binds electrostatically to the amino groups of chitosan (main interaction) and then reduces to Cr(III) compounds [20] (Fig. 8). It has been reported that Cr(VI) is reduced to Cr(III) at pH $\leq$3 by glutaraldehyde molecules (cross-linker) [20]. This is supported by new peaks in FTIR spectra of Cr(VI)-loaded sorbents (*Ch*, 532 cm^{-1}; *Ch-g-Aam*, 535 cm^{-1}; *Ch-g-Aa*, 540 cm^{-1}), suggesting the formation of $Cr(OH)_3$ [49].

3.5. Regeneration

In order to find out the applicability of prepared sorbents in fixed bed configurations, four cycles of sorption–desorption were carried out. Fig. 9a and b shows that the reduction in sorption percentages from the 1st cycle to 4th cycle in the case of *Ch*, *Ch-g-Aam*, *Ch-g-Aa* was: (i) Cu(II), 10%; 13%; 5%; and (ii) Cr(VI) 9%; 4%; 10%. Therefore all the materials can be used repeatedly without any significant loss of their sorptive ability.

4. Conclusions

In this study, three cross-linked chitosan derivatives were used as sorbents for the removal of Cu(II) and Cr(VI) from aqueous solutions: (i) *Ch*, without grafting; (ii) *Ch-g-Aam*, grafted with acrylamide; and (iii) *Ch-g-Aa*, grafted with acrylic acid. The major experimental observations are summarized below:

- *Ch-g-Aa* material presented the highest sorption capacity for Cu(II) removal (318 mg/g at pH 6) among the studied and cited chitosan materials.
- *Ch-g-Aam* material presented the highest sorption capacity for Cr(VI) removal (935 mg/g at pH 4) among the studied and cited chitosan materials.
- Thermodynamic analysis revealed that the sorption of Cu(II) and Cr(VI) onto chitosan was endothermic, spontaneous with an increased randomness.
- The kinetic data were successfully fitted to the phenomenological kinetic model (DIFRE). The calculated diffusion coefficients of Cu(II) and Cr(VI) into sorbents were close to their diffusion coefficients into pure water ($\sim 10^{-10}\ \text{m}^2/\text{s}$).
- The regeneration ability of the loaded chitosan derivatives was tested in four sequential cycles of sorption–desorption presenting a limited loss of capacity; 5% for Cu(II) onto *Ch-g-Aa* and 4% for Cr(VI) onto *Ch-g-Aam*.

Acknowledgement

The financial support received for this study from the Greek Ministry of Education through the research program Pythagoras II is gratefully acknowledged.

References

[1] W.S.W. Ngah, I.M. Isa, Comparison study of copper ion adsorption on chitosan, Dowex A-1, and Zerolit 225, J. Appl. Polym. Sci. 67 (1998) 1067–1070.
[2] E. Guibal, Interactions of metal ions with chitosan-based sorbents: a review, Sep. Purif. Technol. 38 (2004) 43–74.
[3] Y. Kawamura, H. Yoshida, S. Asai, H. Tanebe, Breakthrough curve for adsorption of mercury (ii) on polyaminated highly porous chitosan beads, Water Sci. Technol. 35 (1997) 97–105.
[4] K. Inoue, K. Yoshizuka, Y. Baba, in: C. Gebelein, C. Carraher (Eds.), Biotechnology and Bioactive Polymers, New York, 1994, p. 35.
[5] M. Rhazi, J. Desbrieres, A. Tolaimate, M. Rinaudo, P. Vottero, A. Alagui, Contribution to the study of the complexation of copper by chitosan and oligomers, Polymer 43 (2002) 1267–1276.
[6] P. Chassary, T. Vincent, E. Guibal, Metal sorption on chitosan and derivative materials: a strategy for polymer modification and optimum use, React. Funct. Polym. 60 (2004) 137–149.
[7] Y.S. Yun, D. Park, J.M. Park, B. Volesky, Biosorption of trivalent chromium on the brown seaweed biomass, Environ. Sci. Technol. 35 (2001) 4353–4358.
[8] N.K. Lazaridis, G.Z. Kyzas, A.A. Vassiliou, D.N. Bikiaris, Chitosan derivatives as biosorbents for basic dyes, Langmuir 23 (2007) 7634–7643.
[9] E. Guibal, C. Milot, J.M. Tobin, Metal-anion sorption by chitosan beads: equilibrium and kinetic studies, Ind. Eng. Chem. Res. 37 (1998) 1454–1463.
[10] K.H. Chu, Removal of copper from aqueous solution by chitosan in prawn shell: adsorption equilibrium and kinetics, J. Hazard. Mater. 90 (2002) 77–95.
[11] M.-S. Chiou, H.-Y. Li, Equilibrium and kinetic modeling of reactive dye on cross-linked chitosan beads, J. Hazard. Mater. 93 (2002) 233–248.
[12] C. Gerente, V.K.C. Lee, P. Le Cloirec, G. McKay, Application of chitosan for the removal of metals from wastewaters by adsorption—mechanisms and models review, Crit. Rev. Environ. Sci. Technol. 37 (2007) 41–127.
[13] W.S.W. Ngah, C.S. Endud, R. Mayanar, Removal of copper(II) ions from aqueous solution onto chitosan and cross-linked chitosan beads, React. Funct. Polym. 50 (2002) 181–190.
[14] S.-T. Lee, F.-L. Mi, Y.-J. Shen, S.-S. Shyu, Equilibrium and kinetic studies of copper(II) ion uptake by chitosan-tripolyphosphate chelating resin, Polymer 42 (2001) 1879–1892.
[15] J.C.Y. Ng, W.H. Cheung, G. McKay, Equilibrium studies of the sorption of Cu(II) ions onto chitosan, J. Colloid Interface Sci. 255 (2002) 64–74.
[16] K.C. Justi, V.T. Favere, M.C.M. Laranjeira, A. Neves, R.A. Peralta, Kinetics and equilibrium adsorption of Cu(II), Cd(II), and Ni(II) ions by chitosan functionalized with 2[-bis-(pyridylmethyl)aminomethyl]-4-methyl-6-formylphenol, J. Colloid Interface Sci. 291 (2005) 369–374.
[17] R. Schmuhl, H.M. Krieg, K. Keizer, Adsorption of Cu (II) and Cr (VI) ions by chitosan: kinetics and equilibrium studies, Water SA 27 (2001) 1–8.
[18] P. Udaybhaskar, L. Iyengar, A.V.S.P. Rao, Hexavalent chromium interaction with chitosan, J. Appl. Polym. Sci. 39 (1990) 739–747.
[19] N. Sankararamakrishnan, A. Dixit, L. Iyengar, R. Sanghi, Removal of hexavalent chromium using a novel cross linked xanthated chitosan, Bioresour. Technol. 97 (2006) 2377–2382.
[20] G. Rojas, J. Silva, J.A. Flores, A. Rodriguez, M. Ly, H. Maldonado, Adsorption of chromium onto cross-linked chitosan, Sep. Purif. Technol. 44 (2005) 31–36.
[21] V.M. Boddu, K. Abburi, J.L. Talbott, E.D. Smith, Removal of hexavalent chromium from wastewater using a new composite chitosan biosorbent, Environ. Sci. Technol. 37 (2003) 4449–4456.
[22] M. Rinaudo, A. Domard, Chitin and Chitosan: Sources, Chemistry, Physical Properties and Applications, Elsevier Science Publishers, Essex, UK, 1989, p. 71.
[23] R.A.A. Muzzarelli, Chitin, Pergamon Press, Oxford UK, 1977, p. 356.
[24] APHA, AWWA, WPCF, Standard Methods for the Examination of Water and Wastewater, 20th ed., American Public Health Association, Washington, DC, USA, 1995, p. 20005.
[25] Y.S. Ho, J.C.Y. Ng, G. McKay, Kinetics of pollutant sorption by biosorbents: review, Sep. Purif. Method 29 (2000) 189–232.
[26] A. Findon, G. McKay, H.S. Blair, Transport studies for the sorption of copper ions by chitosan, J. Environ. Sci. Heal. A 28 (1993) 173–185.
[27] O.A.C. Monteiro Jr., C. Airoldi, Some thermodynamic data on copper-chitin and copper-chitosan biopolymer interactions, J. Colloid Interface Sci. 212 (1999) 212–219.
[28] C.A. Eiden, C.A. Jewell, J.P. Wightman, Interaction of lead and chromium with chitin and chitosan, J. Appl. Polym. Sci. 25 (1980) 1587–1599.
[29] R. Maruca, B.J. Suder, J.P. Wightman, Interaction of heavy metals with chitin and chitosan-3 chromium, J. Appl. Polym. Sci. 27 (1982) 4827–4837.
[30] S. Lagergren, About the theory of so-called adsorption of soluble substances, K. Sven. Vetenskapsakad. Handl. 24 (1898) 1–39.
[31] Y.S. Ho, Citation review of Lagergren kinetic rate equation on adsorption reactions, Scientometrics 59 (2004) 171–177.
[32] Y.S. Ho, G. McKay, Pseudo-second order model for sorption process, Process Biochem. 34 (1999) 451–465.

[33] Y.S. Ho, Review of second-order models for adsorption systems, J. Hazard. Mater. 136 (2006) 681–689.
[34] J. Zeldowitsch, Über den mechanismus der katalytischem oxidation von CO an MnO_2, Acta Physicochim. URSS 1 (1934) 364–449.
[35] G.M. Spinks, C.K. Lee, G.G. Wallace, S.I. Kim, S.J. Kim, Swelling behaviour of chitosan hydrogels in ionic liquid–water binary systems, Langmuir 22 (2006) 9375–9379.
[36] C. Tien, Adsorption Calculation and Modeling, Butterworth-Heinemann, Boston, 1994.
[37] G. McKay, Adsorption of dyestuffs from aqueous solutions using activated carbon: an external mass transfer and homogeneous surface diffusion, AICHE J. 31 (1985) 335–339.
[38] S.J. Allen, G. McKay, K.Y.H. Khader, The adsorption of acid dye onto peat from aqueous solution-solid diffusion model, J. Colloid Interface Sci. 126 (1988) 517–524.
[39] W. Press, B. Flannery, S. Teukolski, W. Vetterling, Numerical Recipes. The Art of Scientific Computing, 2nd ed., Cambridge University Press, New York, 1992.
[40] M.R. Unnithan, T.S. Anirudhan, The kinetics and thermodynamics of sorption of chromium(VI) onto the iron(III) complex of a carboxylated polyacrylamide-grafted sawdust, Ind. Eng. Chem. Res. 40 (2001) 2693–2701.
[41] V.C. Srivastava, I.D. Mall, I.M. Mishra, Adsorption thermodynamics and isosteric heat of adsorption of toxic metal ions onto bagasse fly ash (BFA) and rice husk ash (RHA), Chem. Eng. J. 132 (2007) 267–278.
[42] M. Suzuki, T. Fujii, Concentration dependence of surface diffusion coefficient of propionic acid in activated carbon particles, AICHE J. 28 (1982) 380–385.
[43] W.L. Masterton, E.J. Slowinski, C. Stanitski, Chemical Principles, CBS College Publishing, 1983.
[44] P.W. Atkins, Physical Chemistry, 3rd ed., Oxford University Press, Oxford, UK, 1989.
[45] E. Guibal, Y. Jansson-Charrier, P. Saucedo, P. Le Cloirec, Enhancement of metal ion sorption performances of chitosan: effect of the structure on the diffusion properties, Langmuir 11 (1995) 591–598.
[46] Y. Sağ, Y. Aktay, Kinetic studies on sorption of Cr(VI) and Cu(II) ions by chitin, chitosan, and rhizopus arrhizus, Biochem. Eng. J. 12 (2002) 143–153.
[47] M.-Y. Lee, K.-J. Hong, Y. Shin-Ya, T. Kajuchi, Adsorption of hexavalent chromium by chitosan-based polymeric surfactants, J. Appl. Polym. Sci. 96 (2005) 44–50.
[48] V.M.M. Lobo, J.L. Quaresma, Handbook of Electrolyte Solutions, Physical Science Data Series 41, Elsevier, Amsterdam, 1989.
[49] L. Xia, R.L. McCreery, Chemistry of a chromate conversion coating on aluminum alloy AA2024-T3 probed by vibrational spectroscopy, J. Electrochem. Soc. 145 (1998) 3083–3089.